

FLIGHT DYNAMICS OF A PROJECTILE WITH HIGH DRAG RETARDER DEVICES AT SUBSONIC VELOCITIES

A. Dupuis¹ and W. Hathaway²

¹ *Delivery Systems Section, Defense Research Establishment, Valcartier (DREV), 2459, blvd. Pie-XI Nord, Val-Bélair, Québec, Canada, G3J 1X5*

² *Arrow Tech Associates, 1233 Shelburne Road, South Burlington, VT, 05403 USA*

Free-flight tests were conducted in the Defence Research Establishment Valcartier (DREV) aeroballistic range on a projectile with high drag retarder devices at subsonic velocities. All the main aerodynamic coefficients and dynamic stability derivatives were very well determined using the six-degree-of-freedom single- and multiple-fit data reduction techniques. The aeroballistic range data shows that this projectile is dynamically unstable at low angles of attack. The second order pitch-damping coefficient, the yaw axial force term as well as side moments were also reduced. Wind tunnel, Open Jet Facility experimental results and full-scale aircraft free-flight trials were compared with the aeroballistic ones.

INTRODUCTION

The use of very high drag devices on certain projectile configurations offers one the many possibilities in controlling the range of a projectile in flight [1]. The devices could be easily deployed during flight and at certain levels to achieve the desirable range. They also have the extra advantage of being used on low-cost practice rounds to simulate expensive bombs.

To increase the knowledge base of projectiles with high drag devices, DREV conducted aeroballistic range, wind tunnel, open jet facility as well as full scale free-flight trials to study the fundamental aerodynamic phenomena and the flight dynamics associated to this type of control devices. Furthermore, the database generated during this investigation could be used to point out the advantages and disadvantages of such a concept compared to other ones. They also will constitute a test case to validate numerical prediction codes and analytical tools.

MODEL CONFIGURATION

The projectile configuration that was considered is shown in Fig. 1. The projectile has a 1.35 cal ogive nose followed by a 4.07 cal cylindrical portion and four fins are placed at

the end of an 2.48 cal extended boattail. The fins have a 2.00 cal span and they are of a clipped delta type. The fin leading edges are blunt with a thickness of 0.08 cal, which reduces to 0.05 cal at the trailing edge. The fins have no cant to produce spin rate. A high drag 0.07 cal thick retardation disk with a diameter of 1.76 cal is located at 1.89 cal from the nose. A 1.7 cal diameter high drag conical tail is placed just aft of the fins. The reference diameter was 50.8 mm and the center of gravity of the tested projectiles in the aeroballistic range was located at 3.97 caliber from the nose. The total length of the projectile is 8.55 cal.

The nominal physical properties of the model are given in Table I.

EXPERIMENTAL FACILITIES and TEST TECHNIQUES

DREV Aeroballistic Range

The Defense Research Establishment Valcartier (DREV) Aeroballistic Range [2] is an insulated steel-clad concrete structure used to study the exterior ballistics of various free-flight configurations. The range complex consists of a gun bay, control room and the instrumented range. Projectiles of caliber ranging from 5.56 to 155 mm, including tracer types, may be launched. The 230-meter instrumented length of the range has a 6.1-m square cross section with a possibility of 54 instrumented sites along the range (41 for these tests). These sites house fully instrumented orthogonal shadowgraph stations that yield photographs of the shadow of the projectile as it flies down the range. Extraction of the aerodynamic coefficients and stability derivatives is the primary goal in analyzing the trajectories measured in the DREV aeroballistic range. This is done by means of the Aeroballistic Range Data Analysis System (ARFDAS, [3]). The data analysis consists of linear theory, 6 DOF single- and multiple-fit data reduction techniques with the Maximum Likelihood Method.

Eleven (11) projectiles were fired in the aeroballistic range program with the 110-mm smooth bore gun. All the projectiles had roll pins. The muzzle velocities ranged from a low of 270 m/s (Mach 0.8) to a maximum of 323 m/s (Mach 0.95). The mid-range Mach numbers varied from 0.68 to 0.83 that yielded Reynolds number based on the length of projectile, between 6.6×10^6 and 8.0×10^6 , respectively. The initial angles of attack ranged from a low of 1.5° to a maximum of 4.5° . A typical Schlieren photograph showing the complex flow field and shock structure of a projectile in flight can be seen in Fig. 2 for shot A12 at Mach 0.94.

DREV Indraft Wind Tunnel

The wind tunnel experiments were conducted in the DREV trisonic 60 cm x 60 cm wind tunnel [4]. It is an indraft type drawing air into an evacuated tank with a running time of about 6.0 s. Supersonic flow is achieved by the use of interchangeable nozzle blocks. Transonic flow is obtained by the use of a perforated chamber with boundary layer control through suction. Subsonic flow is obtained with one nozzle block with a

downstream choked valve. Standard instrumentation (pitot tubes, wall pressure taps and temperature probes) located in the plenum chamber and in the test section were used to monitor the tunnel free stream conditions. Forces and moments are measured with six component strain gauge balances. The aerodynamic coefficients were obtained by best fit polynomials through the measured experimental data.

DREV Open Jet Facility

The DREV Open Jet Facility (OJF) is a blowdown tunnel [5] having a test section open to the atmosphere. The flow exits through a circular nozzle producing a jet of short duration. Within the core of this jet, the flow is uniform and smooth. The facility consists of a high-pressure reservoir and an interchangeable circular nozzle. The device tested is mounted just downstream of the nozzle. A five-second flow at Mach 0.9 to a 60-second flow (with a 0.9-m nozzle) at Mach 0.3 is possible.

The projectile was free-dropped in the air stream at a Mach number 0.9. The motion was photographed and digitized only in the pitch plane. The three degrees of freedom (X_{cg} , Z_{cg} , and pitch) data is obtained at discrete time intervals. The free-stream aerodynamics as well as interference effects close to the launch platform were determined with OJFDAS [5]. Three projectiles were dropped and analyzed. They were of the same diameter as the aeroballistic range ones but with different physical properties.

Full Scale Drops

The projectile was also air dropped from an aircraft over a Mach number range of 0.3 to 0.9 [6]. The trajectory was obtained from a photo-theodolite system and only the drag coefficient was reduced.

COMPARISON OF RESULTS AND DISCUSSIONS

The static aerodynamic coefficients (C_{X0} , $C_{N\alpha}$ and $C_{M\alpha}$) from the wind tunnel, open jet facility and full scale tests will first be compared with the data obtained from the aeroballistic range. Then the dynamic stability derivatives obtained from the aeroballistic range will be presented. The symbols in the figures are; aeroballistic range single-fit (AB-SF) and multiple fit (AB-MF), the DREV indraft wind tunnel (WT), the Open Jet facility (OJF) and the full-scale tests (FF - M2470). The full-scale tests only provided the total drag coefficient. The results are mostly shown as a function of Mach number. The full analysis of the aeroballistic range results for this configuration is provided in [7] while the results for the projectile with no high drag devices attached are given in [8].

Axial force coefficient

The axial force coefficient at zero angle of attack (C_{X0}) as a function of Mach number is shown in Fig. 3. The aeroballistic range C_{X0} is of the order of 3.5 with a high scatter in the single fit results. The wind tunnel data and the open jet facility results agree extremely well with the aeroballistic range data from Mach 0.7 to 0.9. The full-scale results are slightly above the aeroballistic range results by 15%. It should be noted that full-scale results are for the total C_D and since the projectile flies at a certain limit cycle, it would be expected that the results would be higher than the C_{X0} results. The 2nd order axial force coefficient term, $C_{X\alpha^2}$, was well determined and C_X as a function of angle of attack for the three groups of multiple fits is shown in Fig. 4.

Normal force coefficient slope

$C_{N\alpha}$, the normal coefficient slope, versus Mach number is displayed in Fig. 5. There is a slight scatter in the aeroballistic range single fit results and $C_{N\alpha}$ is about 15.0 over the whole Mach number range tested. The wind tunnel and open jet facility data is within the scatter of the aeroballistic range results.

Pitch moment coefficient slope

The variation of the pitching moment coefficient slope, $C_{M\alpha}$, with Mach number are shown in Fig. 6. There is only a very slight scatter in the aeroballistic range single fit results for $C_{M\alpha}$ and $C_{M\alpha}$ is roughly -50.0 between Mach 0.65 and 0.82. The lone open jet facility data point as well as the wind tunnel results agrees very well with the Mach number range of the aeroballistic range data.

Pitch moment damping coefficient

The tests in the aeroballistic range showed that this configuration is dynamically unstable at low angles of attack over the Mach number range of 0.68 to 0.83 tested. A typical angle of attack history is shown in Fig. 7. All the motion plots [7] show that in most cases the amplitude at 150.0 m downrange was of the order of 6.0° to 8.0° and still increasing but leveling out in some cases. In these aeroballistic range trials, the initial angles of attack were relatively low, roughly 1.5° to 4.5°.

The total pitch-damping coefficient is defined as:

$$C_{Mq} = C_{Mq0} + C_{Mq\alpha^2} \varepsilon^2$$

where ε is the sine of the total angle of attack. The variation of the pitch damping moment coefficient at zero angle of attack, C_{Mq0} , and the second order expansion term, $C_{Mq\alpha^2}$, with Mach number are shown in Fig. 8 and Fig. 9, respectively. C_{Mq0} is positive since the

angular motion increases with range and the very high negative values of $C_{Mq} \alpha^2$ controls the amplitude of the limit cycle. The variation in the numbers are quite high since no final limit cycles were achieved in the short range of the tests and the angular motion keeps increasing.

C_{Mq} as a function of angle of attack for the three multiple data reductions are shown in Fig. 10. As the angle of attack increases C_{Mq} crosses the zero barrier at roughly 3.0° . A dynamic stability analysis [7] showed that the stability bound for C_{Mq} of roughly 39.0. If this stability bound is superimposed on Fig. 10, it can be seen that the cross over point is in the order of 3.0° to 4.0° . This agrees quite well with the motion plots at the mid range value.

Roll damping moment coefficient

Since there were no fin cant on the projectiles, the roll motion was very limited. Therefore, the roll damping moment, C_{lp} , was kept constant -3.9 at the estimates obtained for the projectile with no high drag devices [8]. The roll producing moment due to fin cant, $C_{l\delta}\delta$, was allowed to vary to take into account any manufacturing tolerances in the fin angles.

Other results

A pure side moment (C_{nsm}) was resolved in two multiple shot groups in the aeroballistic range trials. There is no doubt that this side moment originates from the severe turbulence caused by the collar on the fins. The projectile roll motion was almost nil in these cases.

From the aeroballistic range and open jet facility trials, the final limit cycle amplitude was approximated to be between 8.0° to 12.0° .

CONCLUSIONS

The aerodynamic characteristic of projectile with high drag devices at the front and the rear were determined from free-flight tests conducted in the DREV aeroballistic range. Eleven projectiles were successfully fired in the Mach number range of 0.6 to 0.8. The aerodynamic coefficients and stability derivatives (C_{X0} , $C_{N\alpha}$, $C_{M\alpha}$, and $C_{l\delta}\delta$) were well determined. The measured angular motion showed that this projectile is dynamically unstable at low angles of attack. The pitch damping coefficient at zero angle of attack (C_{Mq0}) and the second order expansion term ($C_{Mq} \alpha^2$) were well determined. The yaw axial force term as well as pure side moments and the trims were also reduced. A dynamic stability analysis was also conducted.

Wind tunnel, Open Jet Facility experimental results as well as full-scale tests were compared with the aeroballistic range results. The static aerodynamic coefficients from these three experimental techniques agreed very well with the aeroballistic range data.

From these aeroballistic range tests and the open jet facility experiments, the final limit cycle amplitude of the MPB-HD can be approximated to be between 8.0° to 12.0°.

REFERENCES

1. Higo, S., Takahashi, S., Orita, M., Yamasaki, M., and Uehiro, T., “Experimental and Numerical Study of Aerodynamic Brake”, 18th International Symposium on Ballistics, San Antonio, TX, 15–19 November, 1999
2. Dupuis, A. and Drouin, G., “The DREV Aeroballistic Range and Data Analysis System”, AIAA Paper No. 88-2017, AIAA 15th Aerodynamic Testing Conference, San Diego, California, May 18–20, 1988
3. “ARFDAS97”, Version 4.11, Arrow Tech Associates Inc, August 1997
4. Girard, B., Drouin, G. and Cheers, B., “Supersonic Wind Tunnel Tests (MPBWT-5) of the Modular Practice Bomb”, DREV M 2662/84, June 1984, UNCLASSIFIED
5. “Open Jet Facility Data Analysis System (OJFDAS)”, Arrow Tech Associates Inc., DREV Contract No. W7701-0-1227, March 1992
6. Girard, B., Cheers, B. and Lepage, R., “The Modular Practice Bomb as a Training Simulator for the BL-755 Cluster Bomb”, DREV M 2740/85, August 1985
7. Dupuis, A. D. and Hathaway, W., “Aerodynamic Characteristics of the BDU-5003/B Mod 1 Bomb at Subsonic Velocities from Aeroballistic Range Free-Flight Tests”, DREV-TR-XXXX, in publication
8. Dupuis, A. D., “Aerodynamic Characteristics of the BDU-5002/B Mod 1 Bomb at Subsonic and Transonic Velocities from Aeroballistic Range Free-Flight Tests”, DREV TR 2000–115, November 2000

TABLE I

Nominal physical properties of model

d (mm)	m (g)	I_x (g-cm ²)	I_y (g-cm ²)	l (mm)	CG from nose (cg/l)
50.8	2730.7	10286.1	171702.0	434.34	0.46

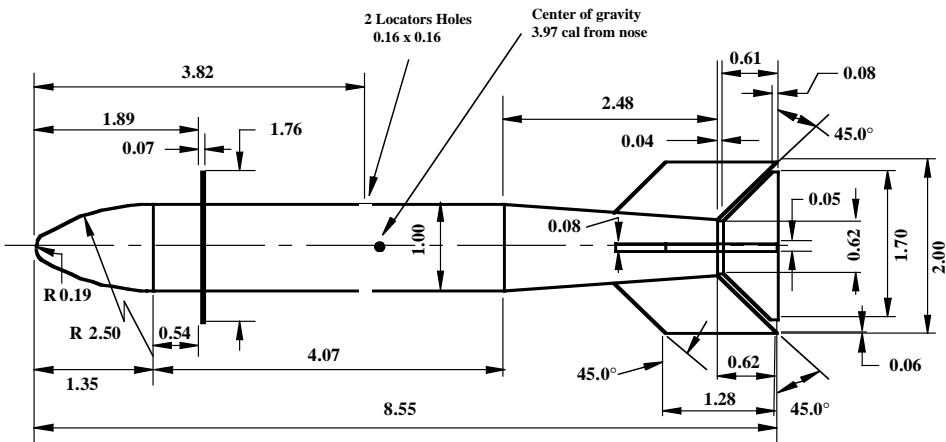


Fig. 1 – Projectile geometry for aeroballistic range tests (all dimensions in caliber).

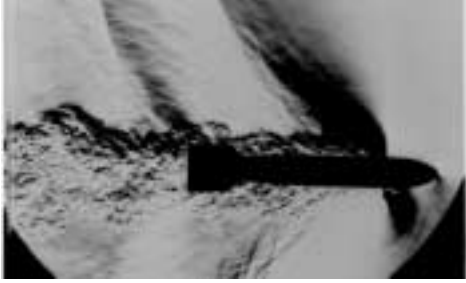


Fig. 2 – Typical Schlieren photograph at $M = 0.9$.

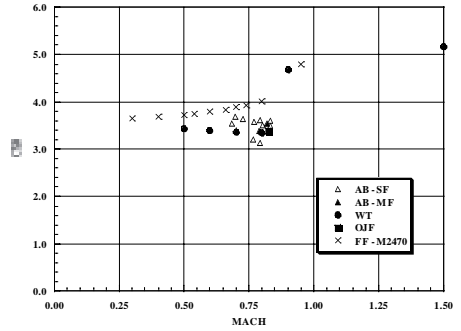


Fig. 3 – Axial force coefficient vs. Mach number.

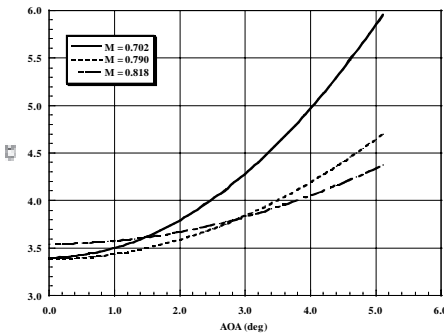


Fig. 4 – C_X versus angle of attack from aeroballistic range data.

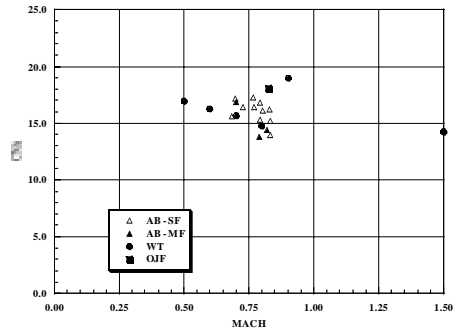


Fig. 5 – Normal force coefficient slope vs. Mach number.

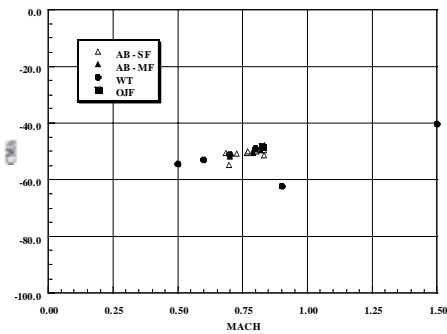


Fig. 6 – Pitch moment coefficient slope vs. Mach number.

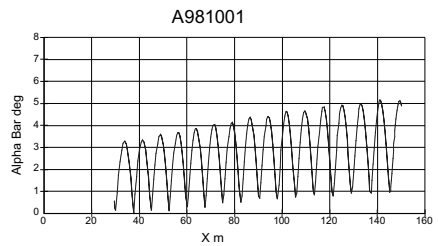


Fig. 7 – Typical angle of attack history.

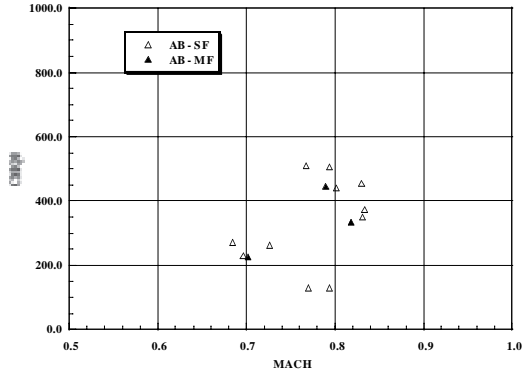


Fig. 8 – C_{Mq0} vs. Mach number.

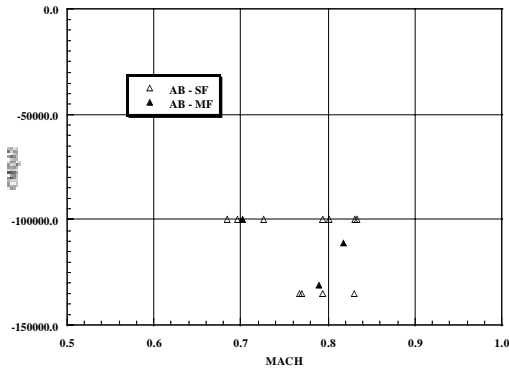


Fig. 9 – C_{Mq0}^2 vs. Mach number.

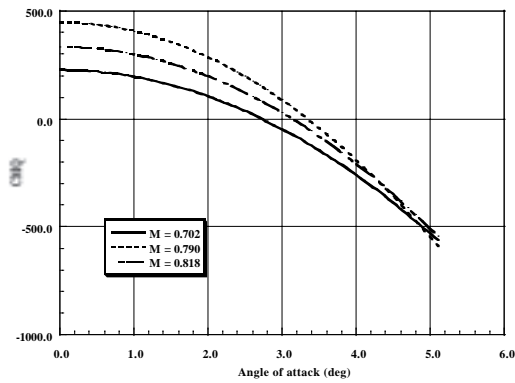


Fig. 10 – C_{Mq} versus angle of attack.